Scientific Research and Essays Vol. 7(38), pp. 3269-3280, 27 September, 2012
Available online at http://www.academicjournals.org/SRE
DOI: 10.5897/SRE12.463
ISSN 1992-2248 ©2012 Academic Journals

Full Length Research Paper

Dynamic modeling and analysis of T-source electronic inverter using state space technique

P. Sivaraman[1]*, A. Nirmal Kumar[2] and P. Prem[1]

[1]Department of Electrical and Electronics Engineering, Bannari Amman Institute of Technology, Sathyamangalam, India.
[2]Department of Electrical and Electronics Engineering, Info Institute of Engineering, Coimbatore, India.

Accepted 16 July, 2012

T-Source inverter is a single stage power converter which can be used as a cost effective alternative for Z-source inverter. Dynamic modeling and analysis of T-source inverter (TSI) is vital for the determination of system limits, components selection for T-shape impedance network and controller design. A novel dynamic model of TSI in continuous conduction mode using the state space approach has been derived here. The derived model has been analyzed by introducing a disturbance in both the load and source side of the TSI. The stability, limitations and component selection of TSI have been done using pole-zero map and frequency response plots. The mathematical models are verified by Matlab / Simulink and experimental results.

Key words: T-Source Inverter, dynamic model, small signal model, state space model, continuous conduction mode.

INTRODUCTION

Nowadays, renewable energy power generation has become more popular due to the depletion of fossil fuel and global warming problems. In renewable energy, the power electronic converters play an important role in converting one form of supply to another form of supply (like DC to DC, DC to AC, etc.) for the generation of power. To overcome the problem of conventional current source inverter (CSI) and voltage source inverter (VSI), (Peng et al., 2005; Peng, 2003) proposed the Z-source inverter. This Z-source has the draw back of high component count and electro magnetic compatibility problem much more than T-source inverter (TSI). Strzelecki et al. (2009) proposed the use of T-source inverter (TSI) (Figure 1) as an interface circuit between source and load. TSI has less reactive components, performs buck boost, and inverts the supply voltage in single stage when compared to other conversion systems power supplied to power converters is not constant at all time because of intermittent potential of wind, solar and fuel cell etc. The end user demand is also varying from time to time. Even though supply voltage is low and intermittent, it is necessary to feed the constant voltage supply to the grid (or) load as it necessitates the need for a controller. To design the proper controller for energy conversion system, it is necessary to study the dynamic behavior of power electronics converters. This paper deals with the dynamic and steady state analysis of T-source inverter (TSI).

Several researchers made an attempt to design the controller for power converters to produce a constant output voltage with variable low voltage input supply. Poh-Chiang et al. (2007) proposed transient modeling, DC and AC analysis of z-source inverter. Quang-Vinh et al. (2007) discussed a new control algorithm to improve the transient response of Z-source converter for fuel cell. Mayo-Maldonado et al. (2010) introduced dynamic analysis of DC-DC multiplier converter for tapping renewable energy based on differential geometry theory. Sen (2010) proposed voltage and current programmed mode controllers which are derived using the ideal small signal model. Large signal black box modeling of three phase voltage source inverter was proposed based on the transient behavior of the converter.

In recent day, dynamic model of a class E inverter with

*Corresponding author. E-mail: sivaramanresearch@gmail.com.

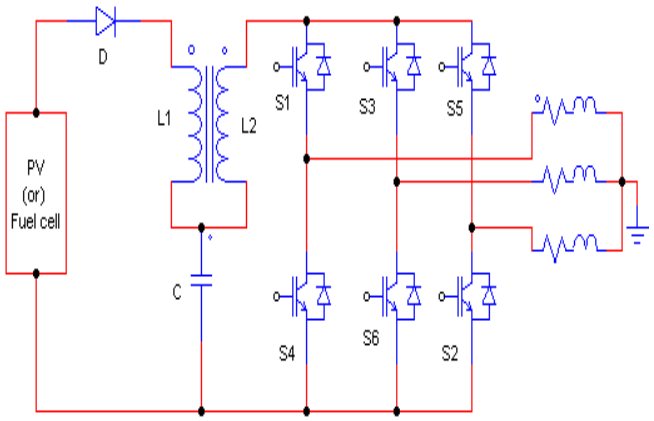

Figure 1. T-Source inverter with variable source.

multi frequency averaged analysis is used for a wide set of analysis and control design tools was proposed by (Carlos et al., 2012; Valdivia et al., 2012) proposed Black-box Modeling of Three-Phase Voltage Source Inverters for System-Level Analysis.. Mohr et al. (2010) presented a study about converting systems for fuel cells which had medium power range and came up with the results that the transformer less inverter gives the best characteristics in terms of system complexity and power loss. Rajakaruna and Jayawickrama (2010) published the steady state analysis and designing impedance network of Z source inverter. This gave guidelines to design the impedance network accurately (Nagaraju et al., 2007).

TSI lacks the detailed dynamic model and analysis since it is a recently proposed topology. But for controller design it is necessary to know the dynamic behavior of converter system. In this paper, dynamic model of T-source inverter is developed using state space averaging techniques and small signal model. The transient and steady state performance of TSI is analyzed for input voltage, duty ratio and load current change with continuous current mode (CCM). The system characteristics are analyzed using frequency dependent transfer function. A prototype of TSI is developed in the laboratory and tested to verify the small signal model.

SMALL SIGNAL MODELING OF TSI

The small signal modeling of power converter is commonly used to study the dynamic characteristics. To develop the small signal model, the following assumptions were made:

1. TSI in continuous conduction mode,
2. L and C in the T network are lossless,
3. Input voltage V_{dc} is independent voltage source and switch S_1 has the forward voltage drop V_D,
4. Switching loss of switch S_2 is neglected,
5. T network L_1=L_2,
6. In active mode of TSI inductor L_2 series with load so I_{L2}=I_L.

The principle of T–source inverter is similar to that of conventional Z-source inverter. When both the switches placed in the same phase leg are turned on, shoot through state occurs. The T network is used as an alternative on the LC-network for boosting the output voltage by inserting shoot through states in the PWM. TSI operates in two modes: (a) Shoot through mode (b) Non shoot through mode.

Figure 2 shows the equivalent circuit of a shoot through mode. Shoot through can be obtained in three different ways such as shoot via one phase leg or combination of two phase legs or combination of all the three phase legs. During this mode, the diode is reverse biased and source is disconnected from the circuit and hence no energy transfer takes place between source to load and vice versa.

In non–shoot through mode, the inverter bridge operate in one of the traditional active state (Shen and Peng, 2004, 2008). The diode conducts and carry differential current between the inductor current and input DC current. Note that both the inductors have an identical current because of coupled inductors. Figure 3 shows the equivalent circuit of a non-shoot through mode.

Dynamic modeling of TSI

Dynamic modeling and analysis for continuous conduction mode (CCM) of Z-Source inverter was done by Jingbo et al. (2007). In T-shape impedance network, source side inductor current (i_{L1}), capacitor voltage (V_c) and load side inductor current (i_{L2}) are the state variables contributing to the state vector for CCM (Krein, 1998) and is defined as

$$\mathbf{x(t)} = \left[\mathbf{i_{L1}(t)\ i_{L2}(t)\ v_c(t)}\right]^{\mathbf{T}} \quad (1)$$

Here, I_{L2}=I_{Load} (load current).

The input voltage V_{dc} is an independent source and load impedance Z_L=R_l+sL_l .from the Equation (1), the state space equation of the shoot through mode can be written as given in Equation (2):

$$\dot{\mathbf{x}}=\mathbf{A_1}.\mathbf{x}+\mathbf{B_1}.\mathbf{u}$$

$$\frac{d}{dt}\begin{bmatrix} i_{L1}(t) \\ i_{L2}(t) \\ v_c(t) \end{bmatrix} = \begin{pmatrix} 0 & 0 & 0 \\ 0 & 0 & -\frac{1}{L_2} \\ 0 & -\frac{1}{C} & 0 \end{pmatrix} \begin{bmatrix} i_{L1}(t) \\ i_{L2}(t) \\ v_c(t) \end{bmatrix} \quad (2)$$

Where $\mathbf{A_1} = \begin{pmatrix} 0 & 0 & 0 \\ 0 & 0 & -\frac{1}{L_2} \\ 0 & -\frac{1}{C} & 0 \end{pmatrix}$ $\mathbf{B_1} = \begin{pmatrix} \mathbf{O} \\ \mathbf{O} \\ \mathbf{O} \end{pmatrix}$

In non–shoot through mode, real energy transfer between the source and load occurs. The equivalent circuit for this mode is as shown in Figure 3. State space equation of the non–shoot through mode is given in Equation (3),

$$\dot{\mathbf{x}}=\mathbf{A_2}.\mathbf{x}+\mathbf{B_2}.\mathbf{u}$$

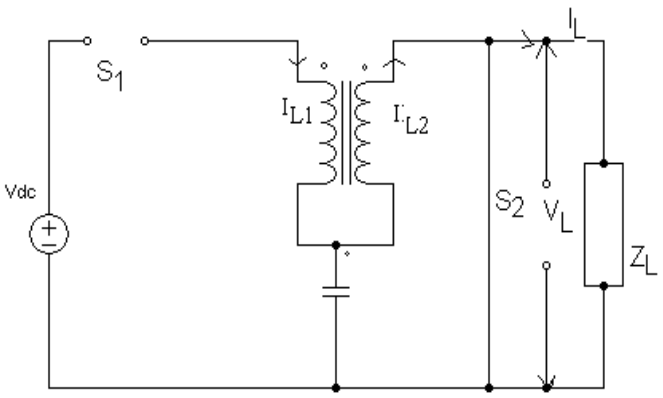

Figure 2. Equivalent circuit of shoot – through mode.

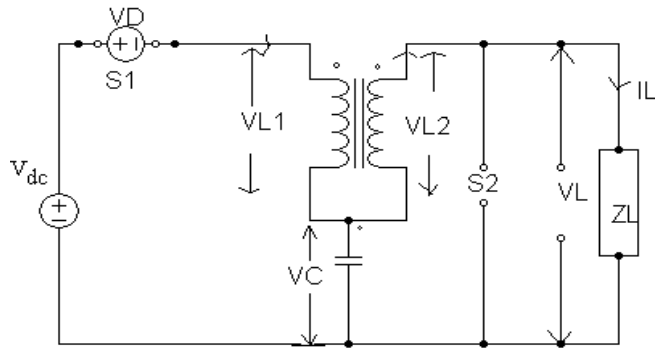

Figure 3. Equivalent circuit of non-shoot through mode.

$$\frac{d}{dt}\begin{bmatrix} i_{L1}(t) \\ i_{L2}(t) \\ v_C(t) \end{bmatrix} = \begin{pmatrix} 0 & 0 & \frac{-1}{L_1} \\ 0 & \frac{-R_l}{L_2(L_2+L_l)} & \frac{-1}{L_2} \\ \frac{1}{C} & \frac{-1}{C} & 0 \end{pmatrix} \begin{bmatrix} i_{L1}(t) \\ i_{L2}(t) \\ v_C(t) \end{bmatrix} + \begin{bmatrix} \frac{1}{L_1} \\ 0 \\ 0 \end{bmatrix} (v_{dc} - v_D) \quad (3)$$

Where

$$A_2 = \begin{pmatrix} 0 & 0 & \frac{-1}{L_1} \\ 0 & \frac{-R_l}{L_2(L_2+L_l)} & \frac{-1}{L_2} \\ \frac{1}{C} & \frac{-1}{C} & 0 \end{pmatrix} \quad B_2 = \begin{pmatrix} \frac{1}{L_1} \\ 0 \\ 0 \end{pmatrix}$$

The relation between small signal state variables is derived by using small perturbation $\hat{v}_{dc}(t)$ to input voltage and $\hat{d}(t)$ to the shoot through duty ratio of S_2 and is given by $V_{dc}(t)=V_{dc}+\hat{v}_{dc}(t)$; $d(t)=D+\hat{d}(t)$; $V_D(t)=0$ and this results in small signal variations in the state variable.

$$x = X + \hat{x}$$

where D is the shoot through duty ratio.

Combining (2) and (3), we get small signal state Equation (4) from Jingbo et al. (2007). It can be rewritten for T-Source inverter as:

$$\hat{\dot{X}}=(D.A_1+D'.A_2).\hat{X}+(DB_1+D'B_2).\hat{U}+(A_1-A_2)X+(B_1-B_2)U \quad (4)$$

$$\begin{pmatrix} L_1 & 0 & 0 \\ 0 & L_2 & 0 \\ 0 & 0 & V_C \end{pmatrix} \frac{d}{dt}\begin{bmatrix} i_{L1}(t) \\ i_{L2}(t) \\ v_C(t) \end{bmatrix} = \begin{bmatrix} 0 & 0 & -D' \\ 0 & -D'R_l & -(D+D') \\ D' & -(D+D') & 0 \end{bmatrix}$$

$$\begin{bmatrix} i_{L1}(t) \\ i_{L2}(t) \\ v_C(t) \end{bmatrix} + \begin{bmatrix} D' \\ 0 \\ 0 \end{bmatrix} (\hat{V}_g(t)) + \begin{bmatrix} V_c - V_g + V_d \\ I_{L2} * R_l \\ -I_{L1} \end{bmatrix} \hat{d}(t)$$

Where the duty ratio of switch S_1 is defined as D' with $D'=1-D$.

Using state space averaging method, the average matrices A and B are:

$$A=D.A_1+D'.A_2 \quad B=D.B_1+D'.B_2$$

From Equation (4), the DC steady state equations following a perturbation can be written as :

$$\begin{bmatrix} 0 \\ 0 \\ 0 \end{bmatrix} = \begin{bmatrix} 0 & 0 & -\frac{D'}{L_1} \\ 0 & \frac{-D'R_l}{L_2(L_2+L_l)} & \left(\frac{D+D'}{L_2}\right) \\ \frac{D'}{C} & -\left(\frac{D'+D}{C}\right) & 0 \end{bmatrix} \begin{bmatrix} \hat{i}_{L1}(t) \\ \hat{i}_{L2}(t) \\ v_C(t) \end{bmatrix} + \begin{bmatrix} \frac{D'}{L1} \\ 0 \\ 0 \end{bmatrix} (v_g - v_D) \quad (5)$$

The DC steady state values also satisfy $I_{L1}=I_{L2}=I_L$ because of T-network symmetry, and from Equation (5), the steady state values are (Wei and Peng, 2011):

$$V_C = D'\left(V_g - V_D\right) \quad (6)$$

$$I_{L1} = \frac{(D+D')I_{l2}}{D'} \quad (7)$$

$$I_{L2} = \frac{(D+D')V_c}{D'R_l} \quad (8)$$

It is noticeable that steady state value of capacitor voltage is determined by shoot through duty ratio. The small signal equivalent circuit is a circuit representative of the derived mathematical model based on Equation (5).

Small signal state [Equation (4)] is written after taking the Laplace transform:

$$s\hat{I}_{L1}(S)=-\frac{D'}{L_1}\hat{V}_C(s)+\frac{D'}{L_1}\hat{V}_g(s)+\left(\frac{V_C}{L_1}-\frac{(V_g-V_D)}{L_1}\right)\hat{d}(s) \quad (9)$$

$$s\hat{I}_{L2}(S)=-\frac{R_l D'}{L_2(L_2+L_l)}\hat{I}_{L2}(s)-\left(\frac{D+D'}{L_2}\right)\hat{V}_C(s)+\left(\frac{R_l I_{L2}}{L_2(L_2+L_l)}\right)\hat{d}(s) \quad (10)$$

$$s\hat{V}_C(s)=\frac{D'}{C}\hat{I}_{L1}(s)-\frac{D+D'}{L_2}\hat{I}_{L2}(s)-\frac{IL_1}{C}\hat{d}(s) \quad (11)$$

TRANSFER FUNCTION MODEL AND SMALL SIGNAL EQUIVALENT CIRCUIT OF TSI

The Transfer function and equivalent circuit of the AC small signal model are obtained using Equations (9), (10) and (11). The small signal model of capacitor voltage (V_c) and inductor current (I_L) is expressed in Equation (12) and (13), respectively.

$$\hat{V}_C(s)=G_{vcg}(s).\hat{V}_g(s)+G_{vcd}(s).\hat{d}(s) \quad (12)$$

$$\hat{i}_L(s)=G_{iLg}(s).\hat{V}_g(s)+G_{iLd}(s).\hat{d}(s) \quad (13)$$

The transfer function G_{vcg} (s) and G_{vcd}(s) is defined as:

$$G_{vcg}(s)=\left.\frac{\hat{V}_C(s)}{\hat{V}_g(s)}\right|_{\hat{d}(S)=0}$$ is the input to capacitor voltage transfer function.

$$G_{vcd}(s)=\left.\frac{\hat{V}_C(s)}{\hat{d}(s)}\right|_{\hat{V}_g(S)=0}$$ is the control of capacitor voltage transfer function.

Input to capacitor voltage transfer function,

$$G_{vcg}(s)=\frac{sD'^2L_1(sL_2+D'R_l)}{s^3L_1L_2C+s^2L_1CD'R_l+s[D'^2L_2-L_1(D+D')^2]+D'^3R_lL} \quad (14)$$

Control to capacitor voltage transfer function,

$$G_{vcd}(s)=\frac{s\{D'L_2(Vc-V_g+V_D)-L_1(D+D')(I_{L2}R_l-IL_1)\}+D'^2R_l(Vc-V_g+V_D)}{s^3L_1L_2C+s^2D'L_1CR_l+s[D'^2L_2-L_1(D+D')^2]+D'^3R_l} \quad (15)$$

$$G_{iLg}(s)=\left.\frac{\hat{i}_L(s)}{V_g(s)}\right|_{\hat{d}_g(S)=0}$$ **Error! Bookmark not defined.**Input to inductor current transfer function

$$G_{iLg}(s)=\frac{sD'C}{s^2L_1C-D'^2} \quad (16)$$

$$G_{iLd}(s)=\left.\frac{\hat{i}_L(s)}{\hat{d}(s)}\right|_{\hat{V}_g(S)=0}$$ Control to inductor current transfer function

$$G_{iLd}(s)=\frac{sC\{(V_C+V_D-V_G)+D'I_L\}}{s^2L_1C-D^2} \quad (17)$$

Figure 4a stand for the equivalent circuit of inductor loop equation and is derived from Equation (9). The term $D' V_g(t)$ and $D' \hat{V}_c(t)$ are dependent on the voltage of TSI and is modeled as dependent source. The equation $\hat{d}(t).(V_C+V_D-V_g)$ is determined only by the duty cycle variation and can be considered as an independent source. Figure 4b represent the small signal representation of capacitor voltage $V_c(t)$ and is constructed using Equation (11). The term $IL_1\hat{d}(t)$ is an independent current source driven by control variations. $D'\hat{i}_L(t)$ and $(D'+D)\hat{i}L_2(t)$ are dependent current sources in the TSI. Small signal equivalent circuit model in Figure 4c represents the load current loop equation obtained from Equation (10) and consists of dependent voltage source controlled by $\hat{d}(t)$.

RESULTS AND DISCUSSION

Simulation of small signal model

To validate the small signal model, simulation had been done using MATLAB/SIMULINK, the following parameters were considered for minimum ripple current (5%) and minimum ripple voltage viz., input voltage (V_{dc}) is 100 V, voltage drop of switch S_1 is 1.3 V, inductance of T-shape impedance network 300 µH, capacitance of T-shape impedance network 360 µF, load resistance of 8.15 Ω, load inductance of 2 mH, shoot through duty ratio 0.2 and switching frequency 10 kHz. Both detailed model and small signal model of inductor current and capacitor voltage are shown Figures 5a, b, 6a and b, respectively and it is clear that the inductor current and capacitor

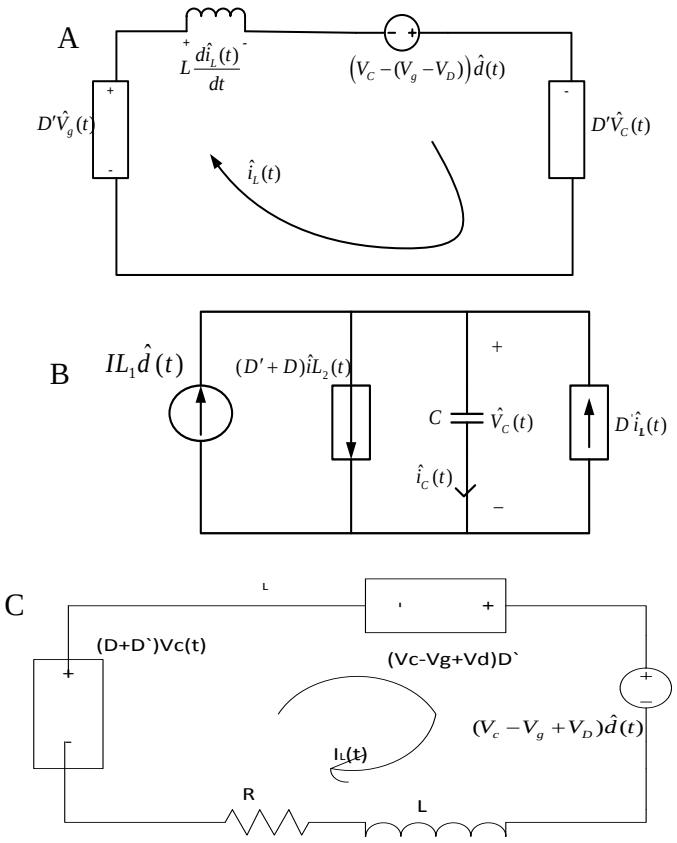

Figure 4. Small signal equivalent circuit model of TSI.

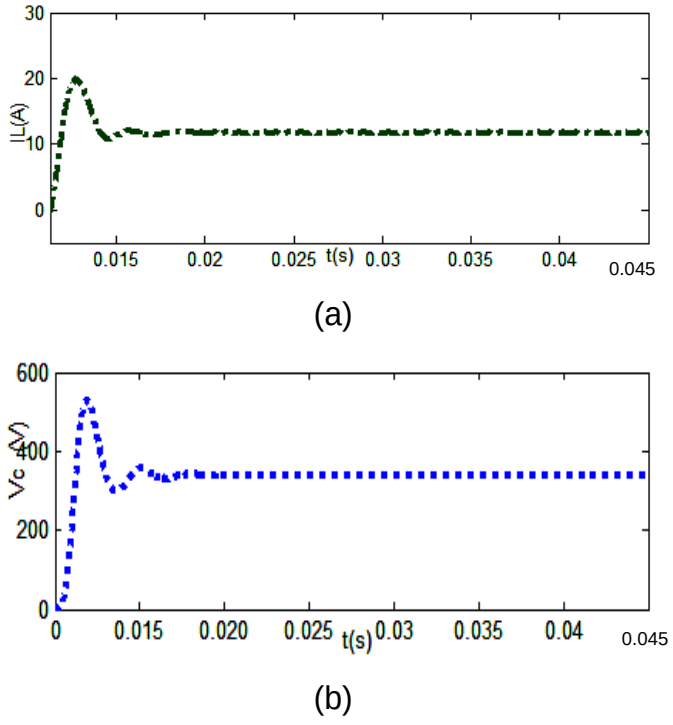

Figure 5. Average circuit model result of TSI (a) inductor current, (b) capacitor voltage.

voltage of small signal model and detailed model has the same dynamic behavior. Over shoot and under shoot in the response shows the current and voltage switching stress across the switch of the TSI.

Design and analysis of T-shape impedance network

The design oriented small signal analysis of TSI had been done to understand the system limits. The performance of TSI transfer function and transient behavior had been analyzed by changing the value of capacitance, inductance and system operating point of T-shape impedance network. Transfer function of small signal model was used to plot the pole–zero (P-Z) map and frequency response of TSI for various values of inductance, capacitance and shoot through duty ratio. The critical values and parameters to design the TSI were thus obtained.

The major advantage of small signal modeling is to find the right half plane (RHP) zeros and poles of TSI transfer function. If the RHP, zeros are present in the pole-zero map the systems tends to be unstable and hence resulting in wide band width feedback loops, striking control limitations and high gain instability occurs.

Effect of inductance in T-network

In order to control the various values of inductance pole-zero map, the capacitor voltage transfer function is plotted as shown in Figure 7. By increasing the value of inductance from100 to 900 µH, the zeros and poles move on the negative real axis towards the origin and the dominant complex pole pair moves towards the origin. The movement of zeros towards RHS increases the non-minimum phase undershoot, at same time shifting of poles increases the system settling time and oscillatory response.

The frequency response is plotted for same value of inductance as shown in Figure 8. From the plot, it is well understood that as inductance increases, phase margin (75.7° to 75.85°) also increases without changes in gain margin (4.3469 db). Comparing the pole zero plot and frequency response, the low value of inductance causes more settling time, whereas high value of inductance causes more overshoot than the other values.

Effect of capacitance variation

The variation in capacitance of control to capacitor voltage transfer function G_{vcd} does not affect the numerator term (that is, zeros are not affected) but affects the denominator term (open loop poles) as shown in Figure 9. It is observed that increasing capacitance results in a small damping factor and the slightly reduced natural frequency of the dominant complex conjugate

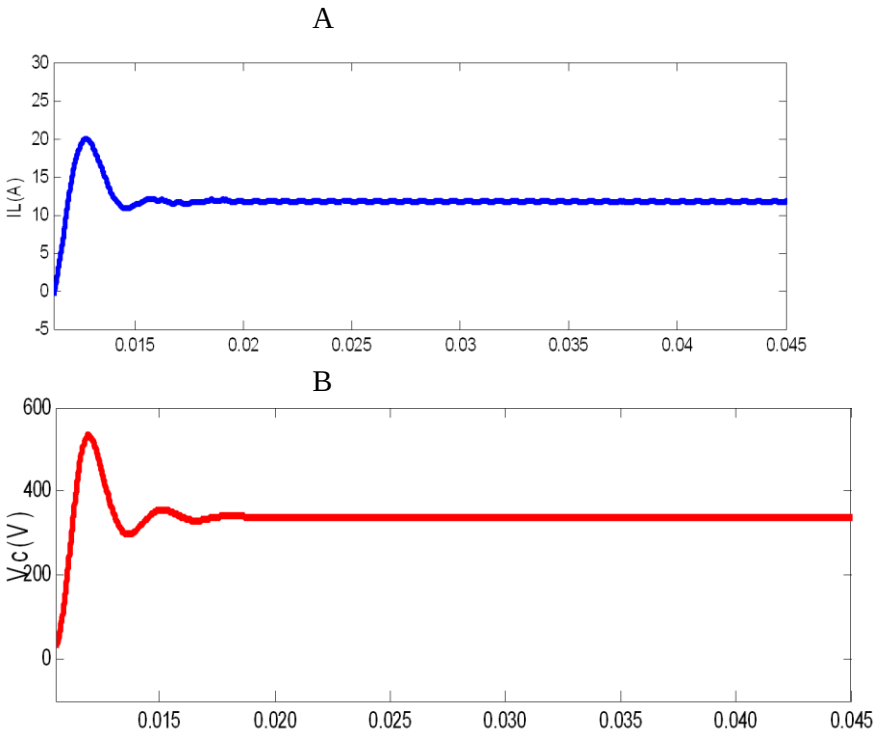

Figure 6. Detailed model result of TSI (a) inductor current, (b) capacitor voltage.

pole pair. Examining from Figure 10, an increase in capacitance causes reduced phase margin with constant gain margin and reduces the natural frequencies of dominant complex conjugate pole pairs. From the pole zero map and frequency response analysis, it is clear that selecting smaller capacitance is more suitable than other choices.

Shoot through duty ratio variation

Shoot through duty ratio is a very useful parameter to find the buck boost capability of TSI. In this part of the paper, pole zero map of control to capacitor voltage transfer function is simulated using the various values of shoot through duty ratio (D) like (0.1, 0.2, 0.3, and 0.4) as shown in Figure 9a. Increasing the value of D moves the poles and zeros towards the origin and dominant pole complex pole pair moves closer to real axis. This shows the high damping, high over shoot and low natural frequency of oscillation. Since real poles and zeros are closer to each other the stability of open loop system will not get affected. The frequency response of the $G_{vcd}(t)$ is plotted for various value of shoot through duty ratio(0.1 to 0.5).It is observed that gain margin and phase margin are initially reduced and then increases as shown in Figure 9b.

The comparison of dynamic simulation with different combination of capacitance (C) and inductance (L) of T-impedance network is as subjected to a step change of shoot through duty ratio from 0.1 to 0.2 as shown in Figure 10.

It is concluded from the results of pole zero plot and frequency response analysis low value of inductance causes large over shoot and high values of L, C and D causes large settling time, high overshoot and reduced resonant frequency. The major drawback is that the quality gets affected as the system also gets oscillated, comparatively. Therefore, in order to mitigate the oscillations, critical values of impedance network are selected. So inductance of the TSI is L_1=L2=300 µH, capacitance is 360 µF and shoot through duty ratio of 0.2 gives less over shoot, quick rise time and less settling time of step response when compared to other values and the same is shown in Figure 10.

Dynamic analysis

From the frequency response and pole zero map analysis, the proper values of T-shape impedance network is selected. In this section, the dynamic behavior of modeled TSI has been tested by changing the load resistance and by drastic changes in the input supply.

Effect of load variations

To study the dynamic characteristics of TSI, sudden load change is introduced at t=0.55 s as represented in

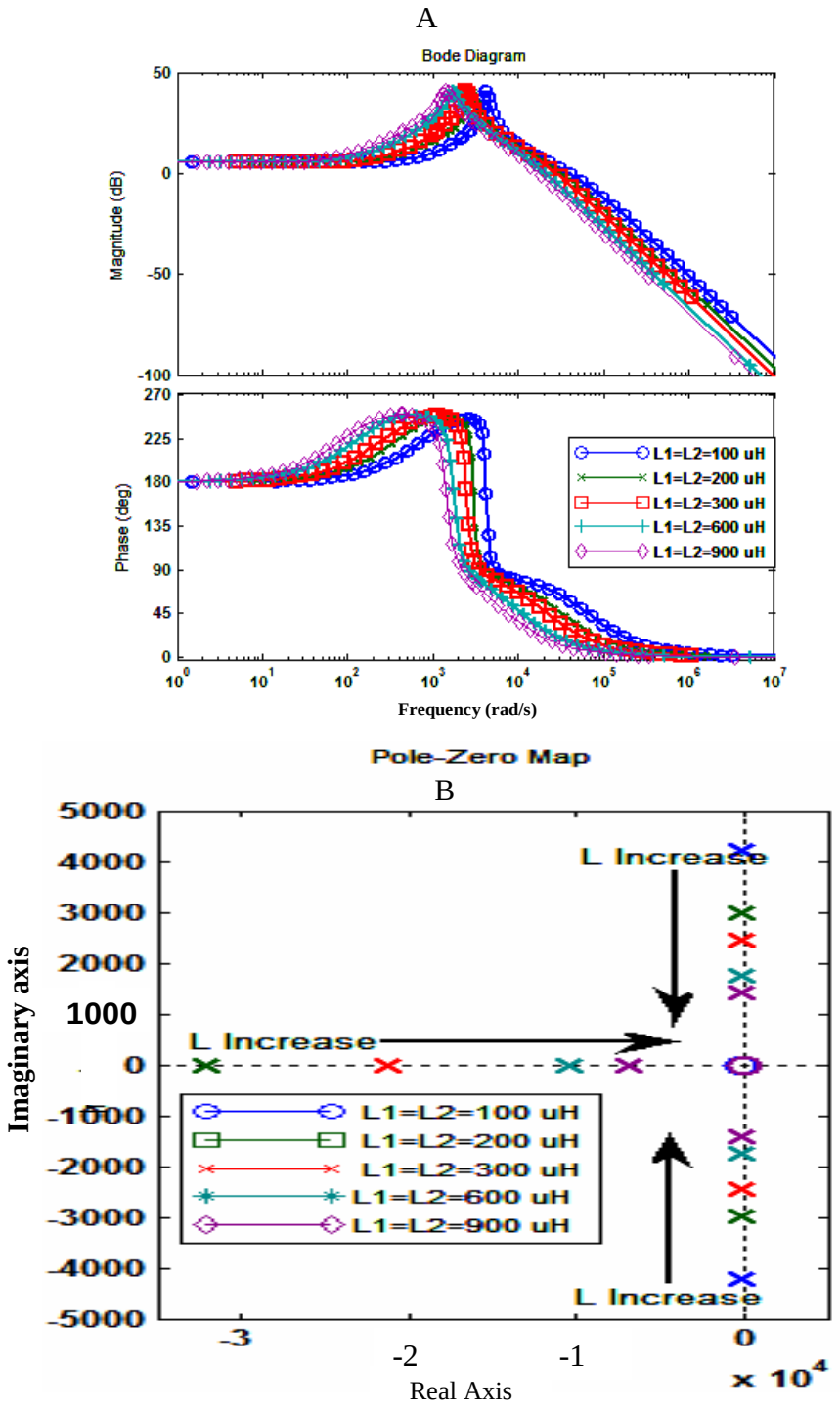

Figure 7. (a) P-Z map and (b) frequency plot of control to capacitor voltage transfer function (G_{vd}) with different inductances.

Figure 11a and b. The sudden increase in the load to 20% from the nominal value will not affect the capacitor steady state value but will affect the quality factor. The output voltage of inverter slightly reduces as the current increases. It shows TSI have good ride through capability.

Effect of input supply variations

Input supply to the TSI is changed to study the dynamic characteristics as shown in Figure 12a, b. At t=0. 27 s, and the sudden increase in input voltage to 20% of nominal value, is observed that the value of DC link

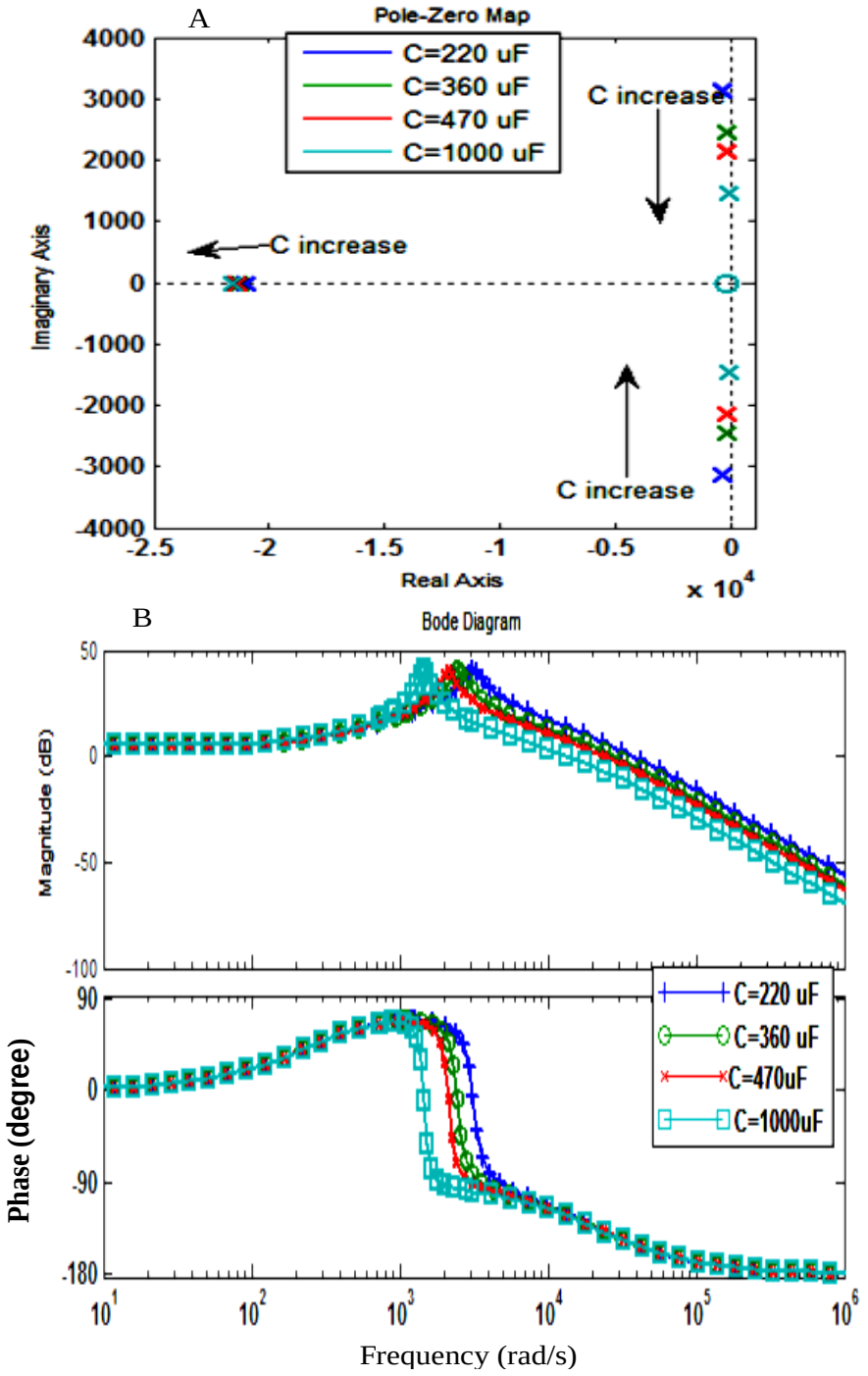

Figure 8. P-Z map of control to capacitor voltage transfer function (G_{vd}) with different capacitances.

voltage get slight overshoot and then reaches a steady state value. The output voltage of inverter is proposanaly increased and current slightly increased. This is due to the presence of RHP zeros in the system. This makes it difficult to get enough phase margins without any overshoot.

Comparison of simulation and experimental results

Based on the previous investigation, simulated results are compared with experimental results. The DC voltage gain of TSI is found for different shoot through duty ratio (D_0) value and represented in Figure 13. Experimental

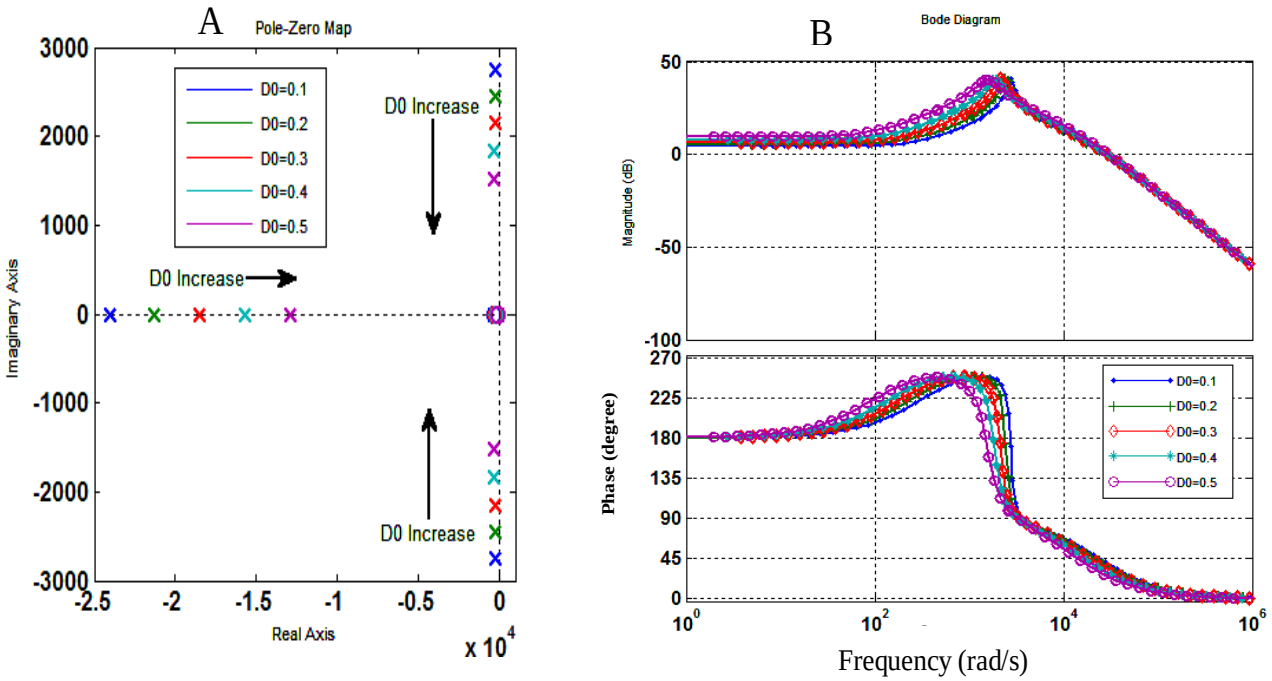

Figure 9. Plot of capacitor voltage transfer function (G_{vd}) with different shoot through duty ratios (a) Pole-Zero plot (b) Frequency response plot.

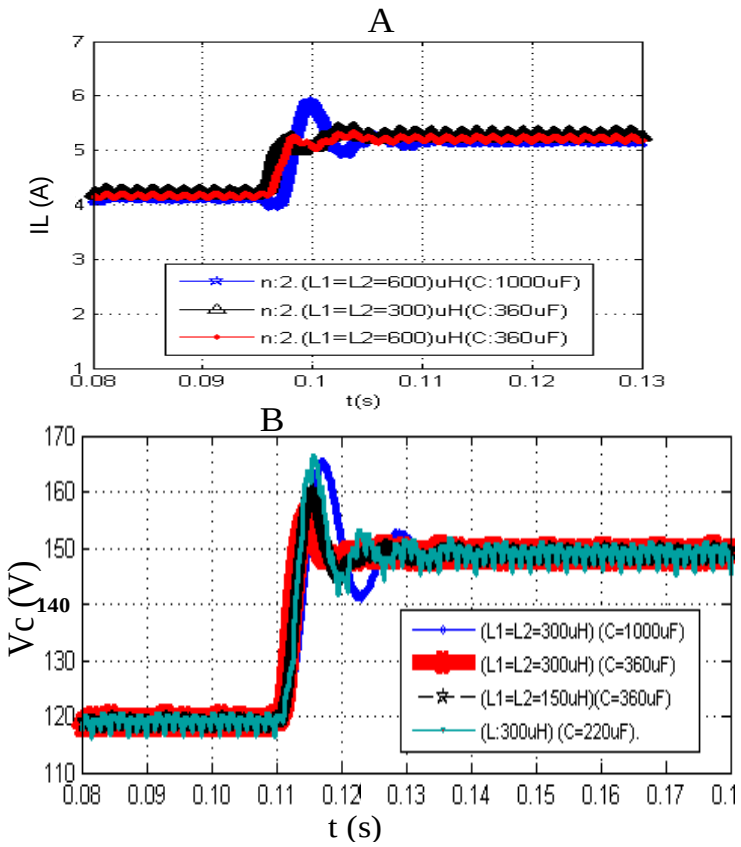

Figure 10. Simulation results of TSI subject to step change of a shoot through duty ratio 0.1 to 0.2 (a) Inductor current (b) capacitor voltage.

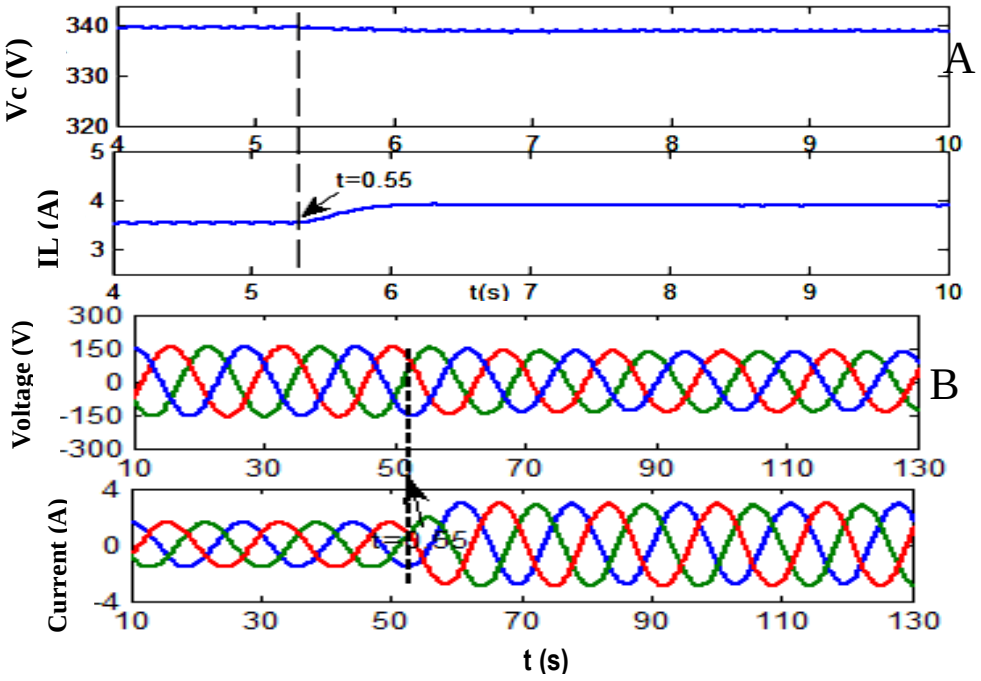

Figure 11. TSI is subject to sudden load change at t=0. 55s.

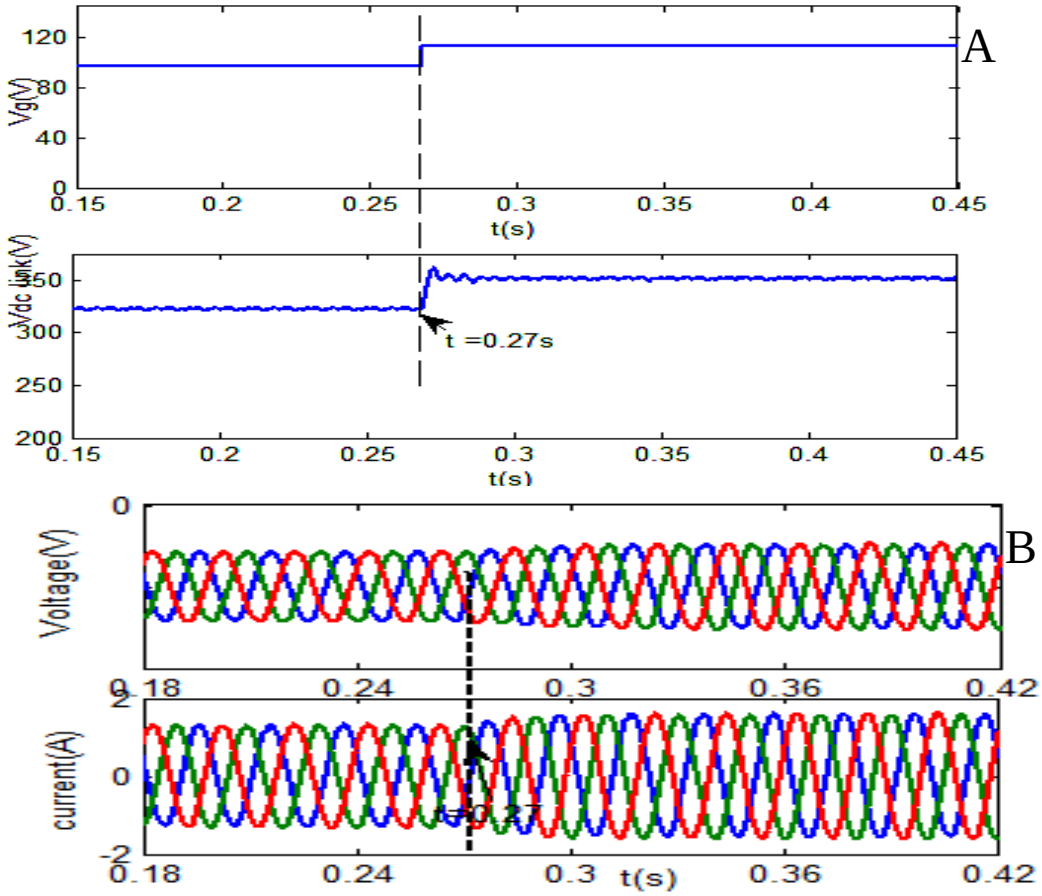

Figure 12. TSI is subject to change in input voltage.

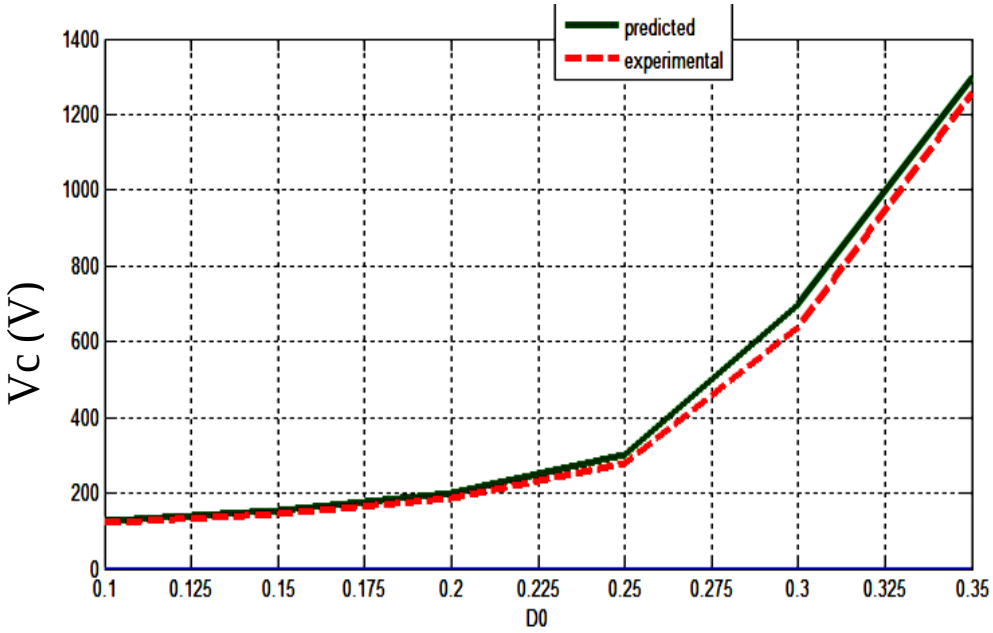

Figure 13. Simulation and experimental results for capacitor voltage V_s shoot through duty ratio.

results were concurrent with their simulated counterpart.

Conclusion

In this work, a small signal model of TSI has been developed. The developed small signal model has been used to obtain the transfer function model of TSI. The critical value of inverter components can be chosen based on the pole zero plots and frequency domain analysis of transfer function model. The results obtained clearly depicts that in open loop condition, TSI is stable under various dynamics such as change in input voltage, change in load current and change in duty ratio.

The critical parameter like inducatance, capacitance, and shoot through duty ratio which were obtained via the pole zero plots and frequency domain analysis can be further used to design a suitable closed loop controller to compensate the voltage dynamics. The Pole-zero maps and the frequency response plot were drawn using MATLAB Simulink software for the obtained transfer function model and is used for parameter selection of T-source impedance network. The future scope for authors will include closed loop control and compensator design and analysis.

ACKNOWLEDGEMENT

The current ongoing study is supported by Bannari Amman Institute of Technology, Department of Electrical and Electronics Engineering, Research Center. We are thankful for their time support and guidance.

REFERENCES

Carlos B, Estanis O, Pilar MG, Arturo M (2012). Dynamic Model of Class E Inverter with Multifrequency Averaged Analysis. IEEE Trans. Ind. Electr. 59(10):3737-3744.

Jingbo L, Jiangang H, Longya X (2007). Dynamic Modeling and Analysis of Z-Source Converter—Derivation of AC Small Signal Model and Design-Oriented Analysis. IEEE Trans. Power Electr. 22(5):1786-1796.

Krein PT (1998). Elements of Power Electronics. New York: Oxford University Press, 1998.

MATLABR2010a,http://www.mathworks.com.

Mayo-Maldonado JC, Salas-Cabrera R, Rosas-Caro JC, Cisneros-Villegas H, Gomez-Garcia M, Salas-Cabrera NE, Castillo-Gutierrez R, Ruiz-Martinez O (2010). Dynamic Analysis of a DC-DC Multiplier Converter. Advances 173:2.

Mohr M, Franke WT, Wittig B, Fuchs FW (2010). Converter Systems for Fuel Cells In the Medium Power Range—A Comparative Study IEEE Trans. Ind. Electr. 57(6):2024-2032.

Nagaraju P, Milan P, Timothy CG (2007). Modeling, Analysis and Testing of Autonomous operation of an Inverter-Based Microgrid. IEEE Trans. Power Electr. 22(2):613-625.

Peng FZ (2003). Z-Source Inverter.EEE transactions on Industry Applications 39 (2): 504-510.

Peng FZ, Shen MS, Qian ZM (2005). Maximum boost control of the Z-source inverter. IEEE Trans. Power Electr. 20(4):833–838.

Poh-Chiang LV, Gajanayake DM, Yih-Rong CJ, Lim-Chern T (2007). Transient Modeling and Analysis of Pulse-Width Modulated Z-Source Inverter. IEEE Trans. Power Electr. 22(2):498-507.

Quang-Vinh T, Tae-Won C, Jung-yol A, Hong-Hee L (2007). Algorithms for Controlling Both the DC Boost and AC Output Voltage of Z-Source Inverter. IEEE Trans. 54(5):2745–2750.

Rajakaruna S, Jayawickrama L (2010). Steady State Analysis and Designing Impedance Network of Z-SourceInverters. Industrial Electronics. IEEE Trans. 57:2483-2491.

Sen GE (2010).Voltage and Current-Programmed Modes in Control of the Z- Source Converter. IEEE Trans. Ind. Appl. 46(2):680–686.

Shen MS, Peng FZ (2004). Maximum constant boost control of the Z-source inverter. In Proc. IEEE-IAS Annu. Meet. pp. 142–147.

Shen M, Peng FZ (2008). Operation Modes and Characteristics of the Z- Source Inverter with Small Inductance or Low Power Factor.

IEEE Trans. Ind. Electr. 55(1):89-96.
Strzelecki R, Adamowicz M, Strzelecka N, Bury W (2009). New type T-Source inverter". Compatibility and Power Electronics, Proc. of 6th Int. Conference-Workshop CPE'09:191-195.
Valdivia V, Lazaro A, Barrado A, Zumel P, Fernandez C, Sanz M (2012). Black-Box Modeling of Three-Phase Voltage Source Inverters for System-Level Analysis. IEEE Trans. Ind. Electr. 59(9):3648-3662.
Wei Q, Fang ZP (2011). Trans-Z-Source Inverters. IEEE Trans. Power Electr. 26(12):3453-3463.